Electronic Supplementary information (ESI)

Substituent effects on fluorescent spin-crossover Fe(II) complexes of rhodamine 6G hydrazones

Juan Yuan,*[a,b] Mei-Jiao Liu,[b] Shu-Qi Wu,[c] Xin Zhu,[a] Nan Zhang,[b] Osamu Sato*[c] and Hui-Zhong Kou*[b]

[a] School of Pharmacy, Henan University of Chinese Medicine, Zhengzhou 450046, P. R. China.

[b] Department of Chemistry, Tsinghua University, Beijing 100084, P. R. China

[c] Institute for Materials Chemistry and Engineering, Kyushu University, 744 Motooka Nishi-ku, 819-0395 Fukuoka, Japan.

E-mail: hnzz_yuan@163.com, kouhz@mail.tsinghua.edu.cn, sato@cm.kyushu-u.ac.jp

Table S1 Magnetic and structural data for $Fe^{II}N_4O_2$ complexes of pyridylhydrazones

Complexes	spin state	$Fe\text{-}N_{imine}$ / Å	$Fe\text{-}N_{pyridyl}$ / Å	Fe-O / Å	*trans*-N-Fe-N angle /°	Ref
$Fe(L^{1})_2$	HS	2.095(2), 2.103(2)	2.264(2), 2.236(2)	2.119(1), 2.083(2)	158.6(7)	28
$Fe(L^{4})_2$	HS	2.079(3), 2.079(3)	2.236(3), 2.204(4)	2.086(3), 2.124(3)	166.7(1)	28
$Fe(L^{5})_2$	HS	2.024(3) ×2	2.083(4) ×2	2.068(3) ×2	174.6(3)	28
$Fe(L^{7})_2$	HS	2.072(2) ×2	2.149(2) ×2	2.082(2) ×2	177.1(1)	29
$Fe(L^{9})_2$	HS	2.101(2) ×2	2.221(2) ×2	2.079(2) ×2	162.48(11)	27
$Fe(L^{10})_2$	HS@290 K	2.112(4), 2.098(4)	2.201(4), 2.206(4)	2.089(4), 2.057(4)	164.72(16)	32
$Fe(L^{10})_2$	HS@315 K	2.097(5)×2	2.213(5) ×2	2.076(4) ×2	165.9(3)	32
$Fe(L^{11})_2$	HS	2.069(4), 2.070(4)	2.190(4), 2.205(3)	2.075(3), 2.085(3)	161.29(14)	31
$Fe_4(L^{13})_4X_4$	HS Fe1	2.101(7), 2.136(7)	2.195(7), 2.202(7)	2.141(5), 2.121(5)	168.5(3)	30
$Fe_4(L^{13})_4X_4$	HS Fe2	2.127(7), 2.105(7)	2.168(7), 2.204(7)	2.124(6), 2.080(6)	171.9(3)	30
$Fe_4(L^{13})_4X_4$	HS Fe3	2.135(7), 2.109(7)	2.139(7), 2.175(7)	2.082(5), 2.145(5)	165.8(3)	30
$Fe_4(L^{13})_4X_4$	HS Fe4	2.136(7), 2.109(7)	2.158(8), 2.193(7)	2.109(5), 2.117(6)	166.8(3)	30
$Fe_4(L^{13})_4X_4$	HS Fe2	2.112(6), 2.066(6)	2.126(6), 2.166(6)	2.081(5), 2.103(5)	170.7(2)	30
$Fe_4(L^{13})_4X_4$	HS Fe3	2.124(6), 2.095(6)	2.172(6), 2.199(6)	2.104(5), 2.144(5)	167.3(2)	30
1	HS@173 K	2.104(5), 2.122(5)	2.245(5), 2.270(5)	2.053(4), 2.069(4)	166.8(2)	This work
$[Fe(L')_2](ClO_4)_2$	HS (93%)	2.093(3), 2.101(3)	2.219(3), 2.244(3)	2.062(2), 2.081(3)	165.05(13)	19
$[Fe(L')_2](ClO_4)_2$	LS (75%)	1.914(3), 1.914(3)	2.059(3), 2.068(3)	1.966(2), 1.962(3)	169.01(12)	19
$Fe(L^{3})_2$	LS (85%)	1.875(2), 1.884(2)	1.966(2), 1.963(2)	1.993(2), 1.975(2)	174.0(1)	28
2	LS	1.852(7), 1.858(7)	1.937(6), 1.956(5)	1.945(4), 1.936(4)	174.2(2)	This work
$Fe(L^{2})_2$	LS	1.864(8), 1.857(8)	1.947(9), 1.915(9)	2.003(7), 1.988(8)	176.5(4)	28
$Fe(L^{5})_2$	LS	1.870(2) ×2	1.946(2) ×2	1.995(2) ×2	176.0(2)	28
$Fe(L^{6})_2$	LS	1.864(2), 1.870(2)	1.927(2), 1.944(2)	1.973(2), 1.985(2)	179.4(0)	28
$Fe(L^{7})_2$	LS	1.888(2) ×2	1.967(2) ×2	1.991(2) ×2	172.4(1)	29
$Fe(L^{8})_2$	LS	1.859(3), 1.876(3)	1.964(3), 1.947(2)	1.996(2), 1.978(2)	178.6(1)	29
$Fe(L^{9})_2\cdot MeOH$	LS	1.864(2) ×2	1.950(2) ×2	1.983(1) ×2	179.07(10)	27
$Fe(L^{10})_2$	LS Fe2	1.865(4), 1.856(4)	1.935(4), 1.945(4)	1.977(4), 1.995(3)	178.77(19)	32
$Fe(L^{10})_2$	LS Fe1	1.865(5) ×2	1.946(5) ×2	1.982(4) ×2	177.9(3)	32
$Fe(L^{10})_2$	LS	1.868(3), 1.868(3)	1.941(4), 1.951(3)	1.966(3), 1.972(3)	179.01(18)	32
$Fe(L^{11})_2$	LS	1.865(2), 1.867(2)	1.960(2), 1.955(2)	2.014(2), 2.015(2)	175.06(7)	31
$Fe(L^{12})_2$	LS	1.833(8) ×2	1.963(7) ×2	1.972(5) ×2	179.1(4)	31
$Fe_4(L^{13})_4X_4$	LS Fe1	1.962(6), 1.909(8)	2.025(6), 2.001(6)	2.014(5), 2.049(5)	170.8(3)	30
$Fe_4(L^{13})_4X_4$	LS Fe4	1.968(6), 1.950(8)	2.020(7), 2.048(6)	2.045(5), 2.047(5)	171.9(3)	30

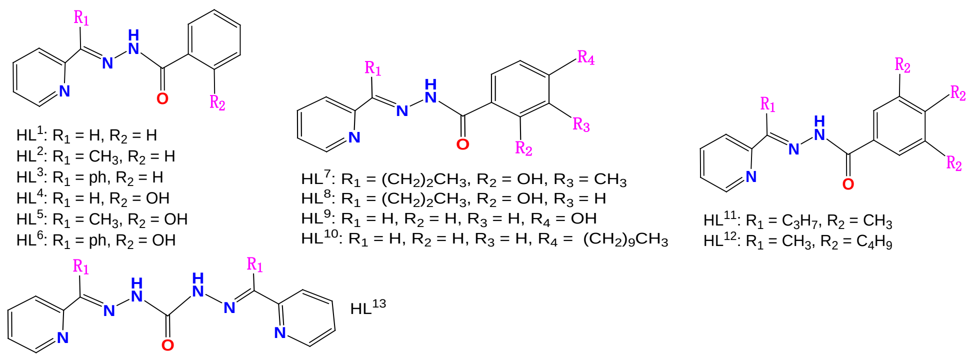

Table S2 Fe-L bond lengths of optimized geometries.

	$[Fe(L^1{}_S(Br))_2]$	$[Fe(L'_S(Me))_2]$	$[Fe(L'(Me))_2]^{2+}$	$[Fe(L^2{}_S(H))_2]$
$Fe\text{-}N_{py}$	2.071 Å, 2.071 Å	2.045 Å, 2.050 Å	2.075 Å, 2.076 Å	1.978 Å, 1.978 Å
$Fe\text{-}N_{imi}$	1.886 Å, 1.881 Å	1.880 Å, 1.884 Å	1.894 Å, 1.893 Å	1.881 Å, 1.881 Å
$Fe\text{-}O_{enol}$	1.983 Å, 1.983 Å	1.973 Å, 1.972 Å	2.003 Å, 2.003 Å	1.963 Å, 1.963 Å

Table S3 3*d*-Centered orbital energies and crystal field splitting energies (in atomic unit, a.u.) in optimized geometries.

	$[Fe(L^1{}_S)_2]$	$[Fe(L'_S)_2]$	$[Fe(L')_2]^{2+\,a}$	$[Fe(L^2{}_S)_2]$
$e_{2g}(2)$	-0.0064	-0.0055	-0.1470	-0.0040
$e_{2g}(1)$	-0.0414	-0.0243	-0.1679	-0.0212
$t_{2g}(3)$	-0.1684	-0.1622	-0.3019	-0.1647
$t_{2g}(2)$	-0.1827	-0.1759	-0.3141	-0.1773
$t_{2g}(1)$	-0.1884	-0.1804	-0.3180	-0.1809
$\Delta_o{}^b$	0.1578	0.1579	0.1593	0.1617

[a] Not simplified molecule. [b] $\Delta_o = E_{av}(e_g) - E_{av}(t_{2g})$.

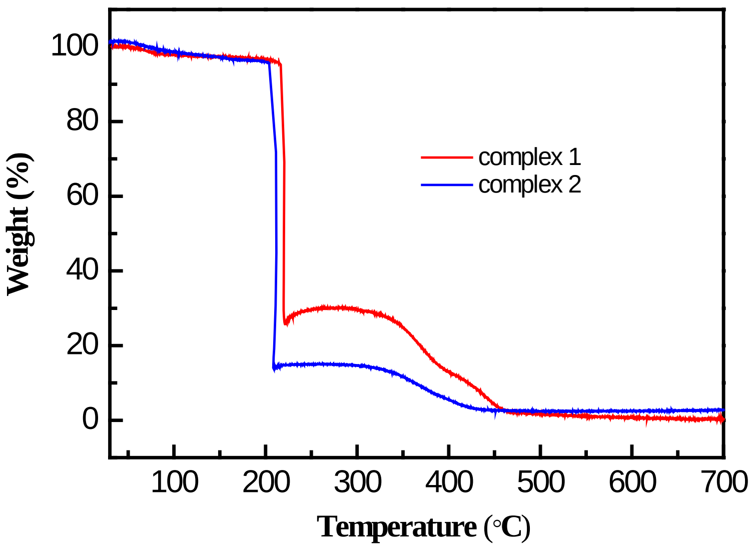

Fig. S1 TGA curve of complexes **1** and **2**.

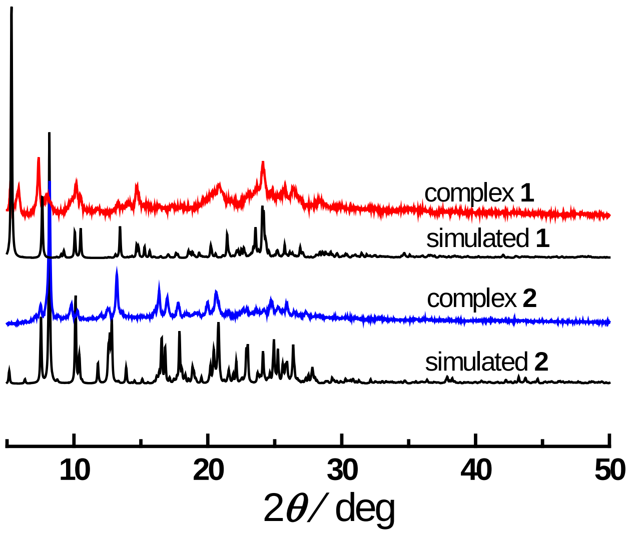

Fig. S2 XRD patterns at room temperature for complexes **1** and **2**.

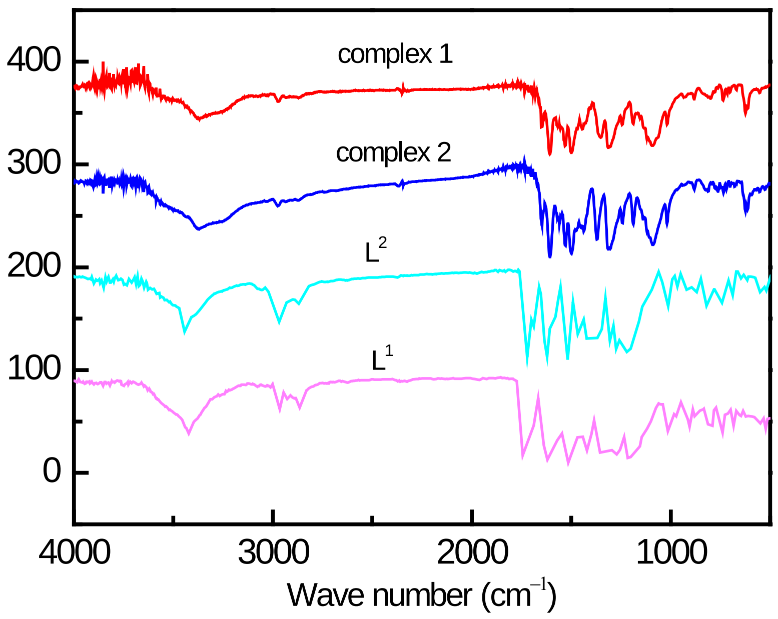

Fig. S3 IR spectra for L^1, L^2 and complexes **1-2**.

$[Fe(L^{1}{}_{s})_2]$ for complex **1**

$[Fe(L^{2}{}_{s})_2]$ for complex **2**

$[Fe(L'_{s})_2]$ for $[Fe(L')_2](ClO_4)_2$

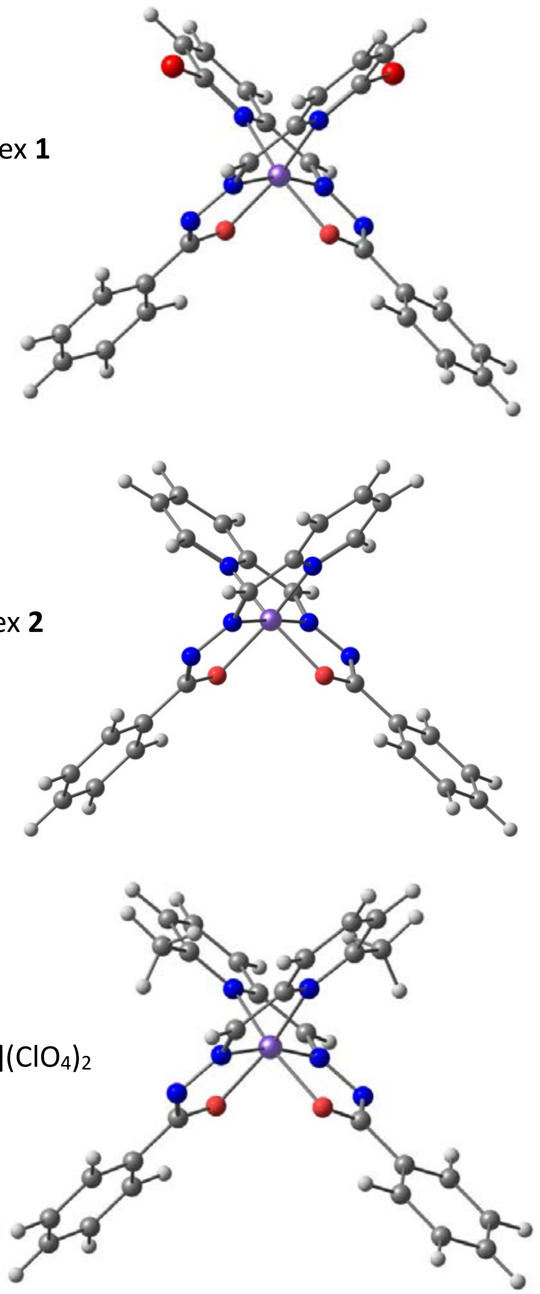

Fig. S4 Optimized model structures for complexes **1**, **2** and $[Fe(L')_2](ClO_4)_2$.

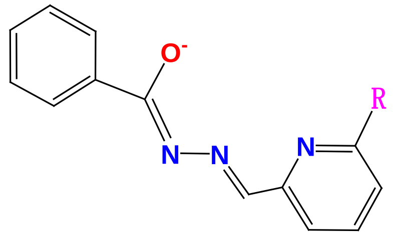

Fig. S5 Simplified structures for the ligands in complexes **1** (R = Br), **2** (R = H) and $[Fe(L')_2](ClO_4)_2$ (R = CH_3).

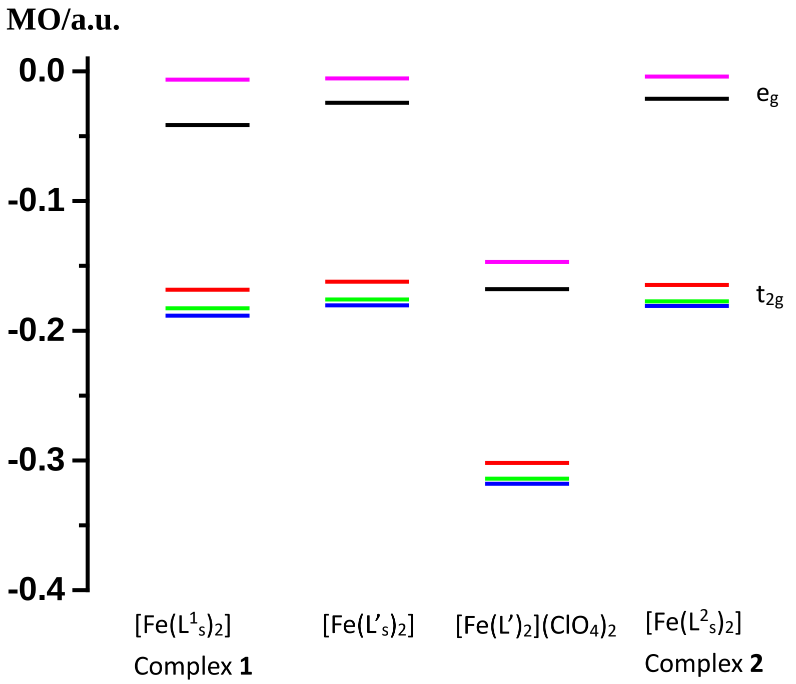

Fig. S6 Energy level in the atomic unit (a.u.) for 3d orbitals of Fe(II) in simplified model complexes **1** (R = Br), [Fe(L')$_2$] (R = Me) and **2** (R = H) as well as [Fe(L')$_2$](ClO$_4$)$_2$ based on the data in Table S3.

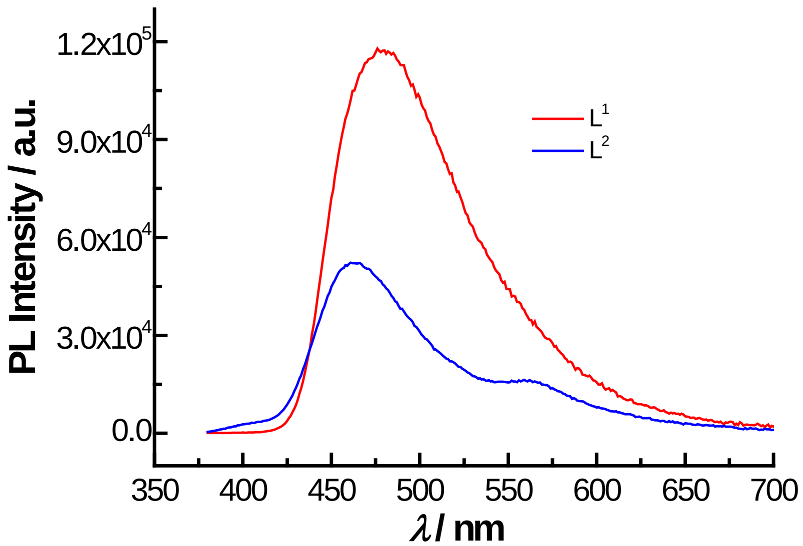

Fig. S7 The emission spectra for ligands L^1 and L^2 in solid state (λ_{ex}= 355 nm) at room temperature.